JEM Journal of Experimental Medicine

BRIEF DEFINITIVE REPORT

# Allergen exposure functionally alters influenza-specific CD4+ Th1 memory cells in the lung

Mikel J. Rüterbusch[1], Brian D. Hondowicz[1], Kennidy K. Takehara[1], Kurt B. Pruner[1], Thomas S. Griffith[2,3,4,5], and Marion Pepper[1]

**CD4+ lung-resident memory T cells ($T_{RM}$) generated in response to influenza infection confer effective protection against subsequent viral exposures. Whether these cells can be altered by environmental antigens and cytokines released during heterologous, antigen-independent immune responses is currently unclear. We therefore investigated how influenza-specific CD4+ Th1 $T_{RM}$ in the lung are impacted by a subsequent Th2-inducing respiratory house dust mite (HDM) exposure. Although naïve influenza-specific CD4+ T cells in the lymph nodes do not respond to HDM, influenza-specific CD4+ $T_{RM}$ in the lungs do respond to a subsequent allergen exposure by decreasing expression of the transcription factor T-bet. This functional alteration is associated with decreased IFN-γ production upon restimulation and improved disease outcomes following heterosubtypic influenza challenge. Further investigation revealed that ST2 signaling in CD4+ T cells during allergic challenge is necessary to induce these changes in lung-resident influenza-specific CD4+ $T_{RM}$. Thus, heterologous antigen exposure or ST2-signaling can drive persistent changes in CD4+ Th1 $T_{RM}$ populations and impact protection upon reinfection.**

## Introduction

Influenza poses a significant global health burden through seasonal epidemics and the threat of emergent pandemic strains. Lung-resident memory CD4+ T cells ($T_{RM}$) generated in response to influenza can provide robust protection upon reinfection (Teijaro et al., 2010, 2011). CD4+ T cells are critical regulators of both B cell and CD8+ T cell responses yet can also provide protection independently of CD8+ T and B cells (Swarnalekha et al., 2021; Son et al., 2021; Belz et al., 2002; Laidlaw et al., 2014). Once these CD4+ T cells take residency, it is unclear how subsequent heterologous pathogen or environmental antigen exposure may impact this population or alter its functionality.

Prior studies demonstrated that the in vivo reactivation of memory CD4+ T helper 1 (Th1) cells in secondary lymphoid organs is restricted by CD4+ T cell cognate recognition of peptide:MHC complexes (Pepper et al., 2010). Whether or not memory cells in the tissues are similarly restricted or how different inflammatory conditions may alter a memory T cell response was not examined (Pepper et al., 2010). Interestingly, work by Paul and colleagues demonstrated that CD4+ Th2 memory cells in the lung could exacerbate subsequent Th2 immune responses to house dust mite (HDM) in a T cell receptor (TCR)–independent manner through IL-33 (Guo et al., 2015). Following sensing of IL-33, these CD4+ Th2 memory cells produced the effector cytokines IL-5 and IL-13 in the absence of TCR signaling and promoted increased eosinophilia and worsened pathology (Guo et al., 2015). While CD4+ T cell expression of ST2, a component of the IL-33R, is canonically attributed to regulatory T cells or Th2-differentiated cells, CD4+ Th1 cells can also express intermediate levels of ST2 and sense IL-33 present in the environment (Blom and Poulsen, 2012; Schmitz et al., 2005). Another IL-1 family member cytokine, IL-18, has also been implicated in prompting similar functional enhancement of CD4+ Th1 responses (Robinson et al., 1997; Jain et al., 2018). Upon sensing of IL-18, CD4+ Th1 cells can produce IFN-γ independently of TCR stimulation when paired with STAT4 induction in vitro (Robinson et al., 1997). Although these studies have investigated how existing Th1 or Th2 CD4+ T cells can be further enhanced by similar environmental cues, it remains unclear how an existing Th1 $T_{RM}$ population can be impacted by subsequent Th2 stimuli, such as common environmental allergens. We therefore sought to define how influenza-specific CD4+ Th1 $T_{RM}$ cells in the lung phenotypically and functionally respond to subsequent allergen exposure and the consequences of these changes in the context of reinfection.

[1]Department of Immunology, School of Medicine, University of Washington, Seattle, WA, USA; [2]Department of Urology, University of Minnesota, Minneapolis, MN, USA; [3]Microbiology, Immunology, and Cancer Biology Ph.D. Program, University of Minnesota, Minneapolis, MN, USA; [4]Center for Immunology, University of Minnesota, Minneapolis, MN, USA; [5]Masonic Cancer Center, University of Minnesota, Minneapolis, MN, USA.

Correspondence to Marion Pepper: mpepper@uw.edu.

## Results and discussion

### $NP_{311–325}$:I-$A^b$–specific and Der p $1_{117–127}$:I-$A^b$–specific $CD4^+$ T cells are not crossreactive or activated by heterologous responses

To answer how lung-resident $CD4^+$ Th1 $T_{RM}$ can be impacted by subsequent exposure to an irrelevant, common environmental allergen, we developed a model system in which we could study non-crossreactive $CD4^+$ T cell populations with different functional outputs: a predominantly Th1-skewed memory population specific for the influenza nucleoprotein (NP; $NP_{311–325}$:I-$A^b$) and a Th2-skewed population specific for the common allergen Der p 1, a protease produced by the HDM *Dermatophagoides pteronyssinus* (Der p $1_{117–127}$:I-$A^b$; Hondowicz et al., 2016; Crowe et al., 2006; Cabrera-Perez et al., 2015). Magnetic bead enrichment of dual tetramer-stained $CD4^+$ T cells, combined with intravascular labeling prior to sacrifice, was performed to identify NP-specific and Der p 1-specific $CD4^+$ T cells in the lung-draining mediastinal lymph node (dLN) and lung parenchyma at various time points following infection and/or allergen administration (Moon et al., 2007; Anderson et al., 2014). In mice that were exposed to HDM, a significant Der p 1–specific, but not NP-specific, $CD4^+$ T cell population was present in the dLN and lungs 4 d after the final HDM dose (Fig. 1, A and C). Conversely, at an acute time point after influenza A/Puerto Rico/8/34 H1N1 (PR8) infection, NP-specific but not Der p 1–specific $CD4^+$ T cells expanded in both tissues compared with cell numbers in naïve mice (Fig. 1, A and C). At neither acute time point were any Der p 1– and NP-specific double positive $CD4^+$ T cells identified, demonstrating that these two epitope-specific populations are not directly crossreactive or expanding in response to the other antigenic insult (Fig. 1 A; Obst et al., 2005).

Although we did not observe crossreactive responsiveness in a heterologous priming environment, $CD4^+$ $T_{RM}$ cells may be more promiscuous and gain responsiveness to a heterologous challenge in an antigen-independent manner (Geginat et al., 2001; Guo et al., 2015). We therefore quantified NP-specific $CD4^+$ T cells in the dLN and lungs at a memory time point after PR8 infection alone or at the same time point (day 43) in mice that were additionally challenged with HDM (Fig. 1 B). There was no significant difference in the number of NP-specific $CD4^+$ T cells identified in either the dLN or lungs of mice that did or did not undergo a subsequent HDM challenge, demonstrating that allergic sensitization and challenge are not sufficient to alter the size of the influenza-induced NP-specific $CD4^+$ $T_{RM}$ population (Fig. 1, B and C). Overall, these data demonstrate that PR8 infection induces a population of NP-specific memory cells in the dLN and lungs that are not numerically enhanced by subsequent HDM exposure.

### HDM-induced airway inflammation following influenza A virus infection decreases the frequency of T-bet–expressing NP-specific $CD4^+$ $T_{RM}$ in the lung

While NP-specific cells did not expand in response to HDM in the dLN or lungs at either acute or memory time points, it was possible that an altered environment associated with airway inflammation could impact functional attributes of the NP-specific memory $CD4^+$ T cells. To test this possibility, we compared hallmark characteristics of NP-specific $CD4^+$ cells from the lungs of mice infected with PR8 alone to those additionally exposed to HDM (Fig. 2 A). Specifically, we analyzed the expression of the lineage-defining transcription factor T-bet as influenza induces a strong Th1 response, characterized by the expression of the T-bet–regulated cytokine IFN-γ (Szabo et al., 2000). As prior studies have suggested that in vivo exposure to IL-33 can enhance $CD4^+$ T cell function in an antigen-independent manner, we also examined expression of ST2 (Löhning et al., 1998; Baumann et al., 2015; Guo et al., 2015).

After PR8 infection, the majority of NP-specific $CD4^+$ $T_{RM}$ cells in the lung express higher amounts of T-bet than naïve antigen non-specific $CD4^+$ T cells (Fig. 2, B and C). Following HDM challenge, however, we observed a lower frequency and level of T-bet expression in the lung-resident NP-specific $CD4^+$ T cell population compared with mice exposed to PR8 alone, suggesting that HDM exposure can diminish T-bet expression in this NP-specific $CD4^+$ $T_{RM}$ population (Fig. 2, B and C). Furthermore, the frequency of NP-specific $CD4^+$ T cells that express ST2 increased after HDM challenge, with this increase occurring primarily in T-$bet^-$ and not T-$bet^+$ cells (Fig. 2, B and C). This finding suggested the possibility that allergic airway inflammation was potentially skewing these Th1 memory cells toward a Th2 lineage as $CD4^+$ Th2 cells express high amounts of ST2 and the Th2-lineage defining transcription factor GATA-3, yet low amounts of T-bet (Van Dyken et al., 2016; Zhang et al., 1997; Finotto et al., 2002). While we could identify a population of bona fide Th2-differentiated Der p 1–specific $CD4^+$ T cells that co-express high levels of GATA-3 and ST2 following HDM exposure, we did not observe GATA-3 expression in NP-specific $CD4^+$ $T_{RM}$ after allergic challenge, suggesting HDM exposure does not direct these cells toward a Th2 fate (Fig. 2, D and E). We additionally did not observe a change in the frequency or level of expression of the regulatory T cell transcription factor Foxp3 in the NP-specific $CD4^+$ $T_{RM}$ population in the lung (Fig. 2, F and G). Thus, although sensitization and heterologous challenge with HDM is not sufficient to induce expansion of NP-specific $CD4^+$ T cells in the lung, the frequency of T-bet and ST2 expressing cells in the NP-specific population is altered without driving these cells toward a Th2 or regulatory $CD4^+$ T cell fate.

While we observed phenotypic and functional alterations in the NP-specific $CD4^+$ T cell population in the lung after HDM exposure, it was unclear whether these changes were a transient response to acute allergic challenge or a longer-term change. Therefore, we waited 25 d after the final allergic challenge to determine if the decreased frequency of T-$bet^+$ NP-specific $CD4^+$ $T_{RM}$ was maintained (Fig. 2 H). We observed that influenza-infected mice that received a subsequent HDM challenge maintained a lower frequency of T-$bet^+$ NP-specific $CD4^+$ $T_{RM}$ in the lung than in HDM-unchallenged mice, suggesting the impact of allergen exposure on the $CD4^+$ $T_{RM}$ population persisted at least this long (Fig. 2, I and J). Of note, the overall frequency of $ST2^+$ NP-specific $T_{RM}$ was not altered in mice that underwent allergic challenge at this later time point, suggesting the increased expression of ST2 on NP-specific $CD4^+$ $T_{RM}$ soon after allergic challenge may be transient (Fig. 2, J and K). Taken together, these data suggest the decrease in T-$bet^+$ NP-specific $CD4^+$ $T_{RM}$ that is seen after HDM exposure persists at least up to 25 d after allergic challenge.

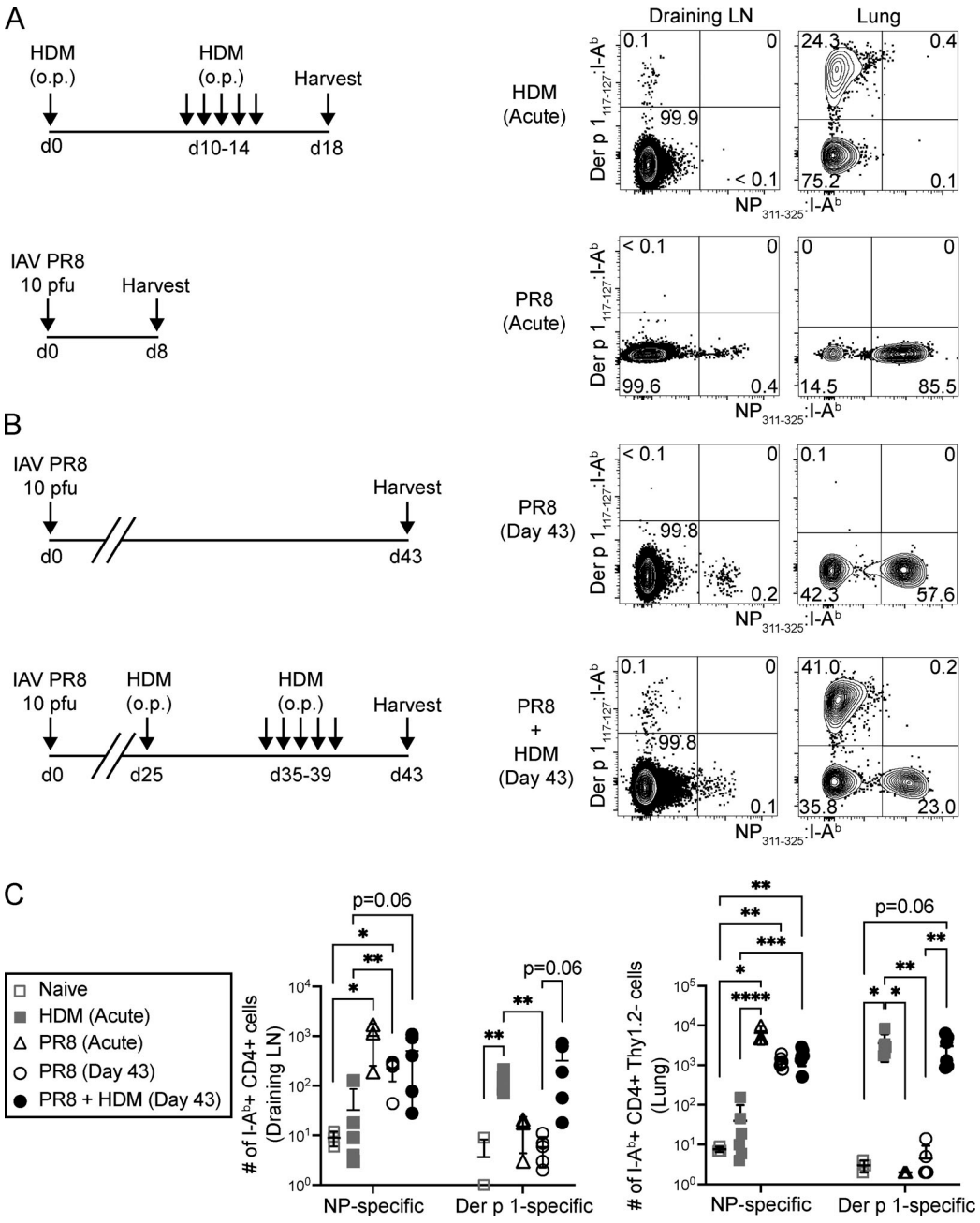


Figure 1. **$NP_{311–325}$:I-$A^b$–specific and Der p $1_{117–127}$:I-$A^b$–specific CD4⁺ T cells are not crossreactive or activated by heterologous responses. (A)** In mice administered respiratory HDM (top) or PR8 (bottom) as illustrated in the experimental timeline shown, lung-draining mediastinal lymph nodes and lung tissues were isolated and stained with Der p $1_{117–127}$:I-$A^b$ and $NP_{311–325}$:I-$A^b$ tetramers and analyzed by flow cytometry. Representative flow plots are shown. Lung samples were pregated on cells that are negative for the intravenous Thy1.2 label to demarcate cells located in the lung parenchyma. **(B)** Representative flow cytometry plots of CD4⁺ T cells isolated from the mediastinal lymph node or lung 43 d after infection with PR8 (top) or following PR8 and respiratory HDM (bottom) as illustrated in the experimental timeline shown. Lung samples were pregated on cells negative for the intravenous Thy1.2 label to demarcate cells located in the lung parenchyma. **(C)** Summary data of the total number of NP-specific or Der p 1–specific tetramer-positive cells in the mediastinal lymph node or lungs of mice from each condition as represented in B. Data are pooled from three to six mice per group from three independent experiments and were analyzed by unpaired *t* test. Graphs show mean ± SD. *, P < 0.05; **, P < 0.01; ***, P < 0.001; ****, P < 0.0001. IAV, influenza A virus. o.p., oropharyngeal. pfu, plaque-forming units.

### NP-specific CD4⁺ $T_{RM}$ in the lung exhibit a decreased potential to produce IFN-γ and IL-10 following allergic sensitization and challenge

Allergen exposure can elicit cytokine production from lung memory CD4⁺ Th2 cells independent of TCR signaling (Guo et al., 2015). We therefore next sought to determine whether HDM can induce effector cytokine production by NP-specific CD4⁺ Th1 memory cells in vivo. To test this, we utilized mice that contained one copy of both an IL-5 protein reporter construct (Red5; IL-5 tdTomato) and an IFN-γ transcriptional reporter construct

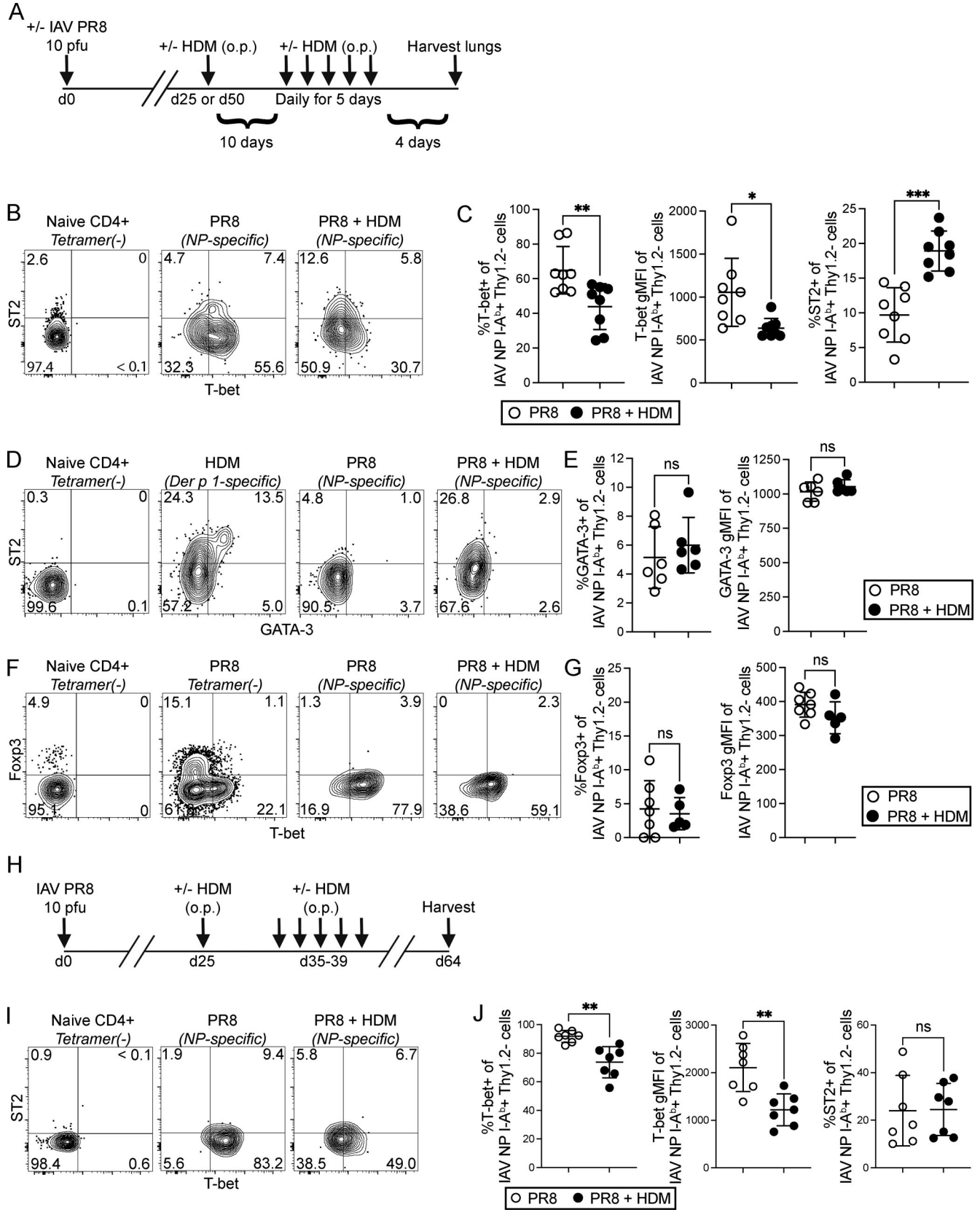


Figure 2. **HDM-induced airway inflammation following influenza A virus infection decreases the frequency of T-bet–expressing NP-specific CD4⁺ $T_{RM}$ in the lung. (A)** Schematic representing the experimental timeline. **(B)** Representative flow cytometry plots of CD4⁺ T cells isolated from the lung at the time point indicated in A. **(C)** Summary data of the percentage of T-bet⁺ NP-specific cells, geometric mean fluorescence intensity of T-bet in NP-specific cells, and the percentage of ST2⁺ NP-specific cells as represented in B. Data are pooled from eight mice per group from two independent experiments.

**(D)** Representative flow cytometry plots of CD4⁺ T cells isolated from the lung at the time point indicated in A. **(E)** Summary data of the percentage of GATA-3⁺ NP-specific cells and geometric mean fluorescence intensity of GATA-3 in NP-specific cells as represented in D. Data are pooled from six mice per group from two independent experiments. **(F)** Representative flow cytometry plots of CD4⁺ T cells isolated from the lung at the time point indicated in A. **(G)** Summary data of the percentage of Foxp3⁺ NP-specific cells and geometric mean fluorescence intensity of Foxp3 in NP-specific cells as represented in F. Data are pooled from five to seven mice per group from two independent experiments. **(H)** Schematic of the experimental timeline for data in I and J. **(I)** Representative flow cytometry plots of CD4⁺ T cells isolated from the lung at experimental day 64. **(J)** Summary data of the percentage of T-bet⁺ NP-specific cells, the geometric mean fluorescence intensity of T-bet in NP-specific cells, and the percentage of ST2⁺ NP-specific cells as represented in I. Data are pooled from seven mice per group from three independent experiments. *, P < 0.05; **, P < 0.01; ***, P < 0.001. Graphs show mean ± SD and data were analyzed by unpaired *t* test. pfu, plaque-forming units. IAV, influenza A virus. o.p., oropharyngeal. gMFI, geometric mean fluorescence intensity.

(Great; IFN-γ YFP; Nussbaum et al., 2013; Reinhardt et al., 2009; Fig. 3 A). In the bulk CD4⁺ T cell population, we could identify IFN-γ⁺ cells in the lungs following infection with PR8, and distinct populations of IFN-γ– and IL-5–producing cells in mice exposed to PR8 and HDM (Fig. 3 B). In the NP-specific CD4⁺ T cell population, IFN-γ transcript was expressed in a majority of these cells after PR8 infection, with a higher level of expression during acute infection than at a memory time point (Fig. 3, B and C). IL-5 expression in NP-specific CD4⁺ T cells was absent at either time point following PR8 infection, further demonstrating this population does not consist of Th2-differentiated cells (Fig. 3, B and C). Notably, we did not observe changes in the frequency or levels of IFN-γ or IL-5 reporter expression in NP-specific CD4⁺ T cells in the lungs of mice additionally exposed to HDM, suggesting NP-specific CD4⁺ Th1 $T_{RM}$ do not alter their expression of these cytokines following allergen exposure (Fig. 3, B and C).

While we did not observe induction of effector cytokine production in NP-specific CD4⁺ $T_{RM}$ after allergen exposure, we sought to assess if the observed decrease in T-bet expression seen after allergen exposure altered cytokine production following reactivation. We therefore isolated NP-specific CD4⁺ memory T cells from the lungs of mice and stimulated them with a protein kinase C activator (PMA) and calcium ionophore (ionomycin) and performed intracellular cytokine staining for effector cytokines consistent with Th1, Th2, and regulatory T cell lineages (Fig. 3 D). While about 50% of NP-specific CD4⁺ $T_{RM}$ from mice infected with PR8 possessed the capacity to produce IFN-γ upon restimulation, NP-specific cells isolated from the lung after induction of airway inflammation produced approximately twofold less IFN-γ (~28%) at the same time point after infection (Fig. 3, E and F). Consistent with the transcription factor profile in these cells, we did not observe expression of the Th2 cytokine IL-13 in NP-specific CD4⁺ $T_{RM}$ but noticed a small, yet statistically significant reduction in IL-10 production after HDM exposure (Fig. 3, G and H). Therefore, decreased T-bet expression in NP-specific CD4⁺ T cells upon allergen exposure is also associated with a decreased frequency and level of IFN-γ expression and concomitant reduction in IL-10 production upon PMA-ionomycin–induced reactivation.

### NP-specific CD4⁺ $T_{RM}$ in HDM-exposed mice maintain decreased T-bet expression after heterosubtypic infection

Although it was clear that HDM exposure could alter the frequency of T-bet expression in NP-specific CD4⁺ $T_{RM}$, it was possible that a subsequent influenza infection could restore T-bet levels in this population. To test this, we utilized influenza A/HKx31 H3N2 (X31) for our heterosubtypic challenge as this strain contains the six internal genes of PR8 including NP, therefore preserving many major CD4⁺ T cell epitopes while evading sterilizing immunity generated during PR8 infection (Rutigliano et al., 2014). Following PR8 infection, mice were either left unchallenged or sensitized and challenged with HDM (Fig. 4 A). On day 50 after PR8 infection, these mice were infected with X31 under FTY720 (Fingolimod) treatment to determine the impact of reinfection and TCR stimulation on the phenotypic changes in NP-specific CD4⁺ $T_{RM}$ observed after HDM sensitization and challenge (Fig. 4 A). FTY720 prevents CD4⁺ T cell migration to the peripheral tissues via degradation of S1PR1 and was sufficient to induce lymphopenia and prevent entry of NP-specific CD4⁺ T cells during X31 infection in our model (Mandala et al., 2002; Fig. 4, B–D). Thus, the NP-specific CD4⁺ T cell population in the lung analyzed at this time point primarily consists of cells present in the tissue prior to heterosubtypic infection and not newly recruited CD4⁺ T cells.

Using this experimental protocol, we observed that following X31 infection, 87–96% of NP-specific CD4⁺ $T_{RM}$ in the lungs expressed T-bet in mice that received a prior PR8 infection but were not challenged with HDM (Fig. 4, E and F). However, the NP-specific CD4⁺ $T_{RM}$ cell population in the lungs of mice that were also exposed to HDM retained a reduced frequency and level of T-bet expression compared with mice that did not undergo allergic challenge even after X31 infection, although the overall frequency of ST2 expression in the NP-specific $T_{RM}$ was lower in HDM exposed mice at this time point (Fig. 4, E and F). Thus, in addition to mice exhibiting a reduced frequency of T-bet⁺ NP-specific CD4⁺ T cells that persisted after challenge with HDM, this change in the NP-specific CD4⁺ $T_{RM}$ population in the lung was maintained after heterosubtypic influenza infection and perception of cognate antigen.

### HDM-exposed mice exhibit improved disease outcomes in response to heterosubtypic infection

Expression of T-bet in CD4⁺ T cells is necessary for IFN-γ production, which has been classically associated with protection against heterosubtypic infection (Szabo et al., 2000; Teijaro et al., 2010). Yet, recent studies have demonstrated that heightened Th1 antiviral responses during influenza infection can induce immunopathology and worsen disease (Schmit et al., 2022; Califano et al., 2018). IFN-γ–deficient mice exhibit lower morbidity, viral load, and improved survival upon lethal influenza infection, which has been attributed to enhanced lung injury through IFN-γ–dependent monocyte activation and ILC2

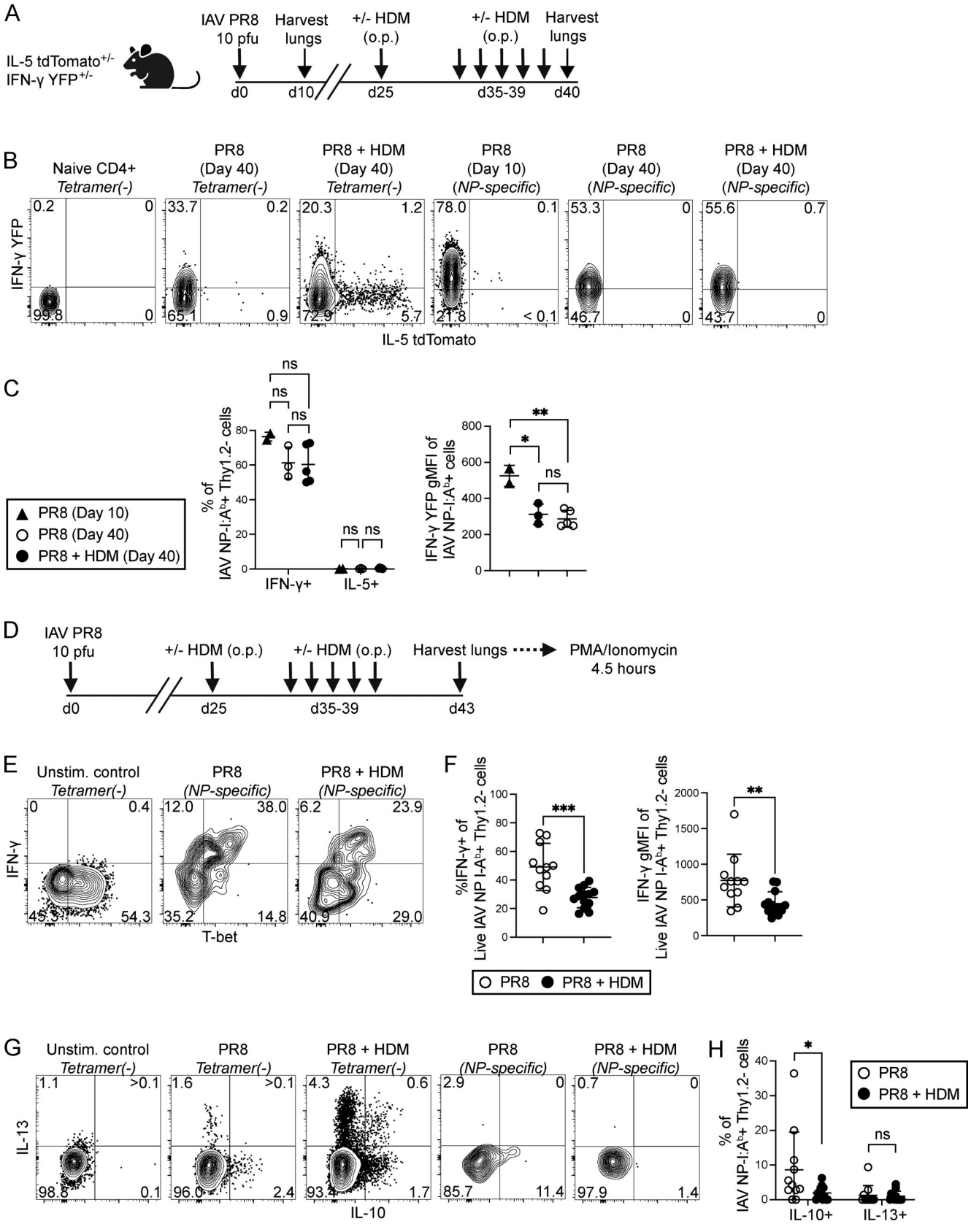


Figure 3. **NP-specific CD4⁺ $T_{RM}$ in the lung exhibit a decreased potential to produce IFN-γ and IL-10 following allergic sensitization and challenge.** **(A)** Schematic of the experimental timeline for data in B and C. **(B)** Representative flow cytometry plots of CD4⁺ T cells isolated from the lung at experimental day 10 or day 40. **(C)** Summary data of the percentage of YFP⁺ or tdTomato⁺ NP-specific cells and the geometric mean fluorescence intensity of YFP in

NP-specific cells as represented in B. Data are pooled from two to five mice per group from two independent experiments. **(D)** Schematic of the experimental timeline for data in E–H. **(E)** Representative flow cytometry plots of CD4⁺ T cells isolated from the lung at experimental day 43 and either incubated in media (unstimulated control) or stimulated with PMA/ionomycin for 4.5 h to assess cytokine production potential. **(F)** Summary data of the percentage of IFN-γ⁺ NP-specific cells and the geometric mean fluorescence intensity of IFN-γ in NP-specific cells as represented in E. Data are pooled from 11–13 mice per group from three independent experiments. **(G)** Representative flow cytometry plots of CD4⁺ T cells isolated from the lung at experimental day 43 and either incubated in media (unstimulated control) or stimulated with PMA/ionomycin for 4.5 h to assess cytokine production potential. **(H)** Summary data of the percentage of IL-10⁺ or IL-13⁺ NP-specific cells as represented in G. Data are pooled from 11–13 mice per group from three independent experiments. *, P < 0.05; **, P < 0.01; ***, P < 0.001. Graphs show mean ± SD and data were analyzed by unpaired *t* test. pfu, plaque-forming units. IAV, influenza A virus. o.p., oropharyngeal. gMFI, geometric mean fluorescence intensity.

suppression (Schmit et al., 2022; Califano et al., 2018). We thus sought to determine if the decreased frequency of T-bet⁺ NP-specific CD4⁺ $T_{RM}$ we observed in HDM-exposed mice that was maintained following X31 infection impacted disease outcomes.

To assess this, we tracked weight loss daily and measured viral load in the lungs 5 d following X31 infection under FTY720 treatment, which prevents the recruitment of novel cell populations to the lungs (Fig. 4, G and H). Mice that underwent allergic sensitization and challenge without a prior PR8 infection exhibited nearly identical weight loss to mice infected with X31 alone until day 5 after infection and possessed no significant difference in viral load in the lung at this time point, demonstrating that HDM exposure alone does not impact early measures of disease upon infection with X31 (Fig. 4, G and H). Prior infection with PR8 reduced weight loss as early as day 3 after X31 challenge and led to decreased viral load on day 5 after challenge, illustrating the protective capacity of memory cells generated in response to PR8 infection (Fig. 4, G and H). However, mice sensitized and challenged with HDM following PR8 infection exhibited even less weight loss starting on day 3 after X31 and possessed lower viral load after heterosubtypic challenge than mice exposed to PR8 but not HDM (Fig. 4, G and H). Therefore, HDM exposure improves early disease severity and viral clearance after influenza infection by impacting the lung-resident memory compartment.

A number of cytokines have been associated with increased weight loss following influenza infection, namely IL-6, TNF-α, and IFN-γ (Schmit et al., 2022; Califano et al., 2018; Felgenhauer et al., 2020). Thus, we assessed the expression of these cytokines in the lung tissue 5 d following heterosubtypic challenge (Fig. S1 A). We observed that mice exposed to HDM following PR8 infection exhibit reduced *Ifng* and *Il6*, but not *Tnf*, expression after X31 infection compared with mice not challenged with HDM, suggesting that allergic sensitization and challenge impacts the memory compartment and leads to reduced expression of these proinflammatory cytokines (Fig. S1 B). We also observed that there was a significant positive correlation between *Il6* expression, *Ifng* expression, the level of T-bet expression in NP-specific CD4⁺ $T_{RM}$, and viral load on day 5 after X31 infection, further demonstrating the association between heightened Th1 responses and worsened disease parameters following influenza infection as has previously been described (Fig. S1 C). In summary, in mice previously infected with PR8, additional exposure to HDM impacts the lung-resident memory compartment and leads to lower expression of proinflammatory cytokines, which correlates with lower viral burden after heterosubtypic influenza challenge.

### Diminished T-bet expression in NP-specific CD4⁺ $T_{RM}$ in the lung can be driven by IL-33 and is dependent on ST2 signaling in CD4⁺ T cells

Immune cell activation following exposure to HDM is attributed to several compounds excreted by the dust mite, including cysteine proteases that promote cleavage of epithelial cell tight junctions and stimulate the release and processing of the alarmin IL-33 (Wan et al., 1999; Scott et al., 2018). Along with these proteases, excrement from HDM contains lipopolysaccharide (LPS), which is a potent inducer of IL-12 and the IL-1 family member cytokine IL-18 (Valerio et al., 2005; Daan de Boer et al., 2013; Manigold et al., 2000; Mantovani et al., 2019). NP-specific CD4⁺ $T_{RM}$ in the lungs of mice can express the receptors for IL-33 and IL-18, the latter of which increases in expression in response to LPS but not papain (Fig. S2, A and B). As the cytokines IL-33 and IL-18 have been implicated in promoting effector functions in memory CD4⁺ T cells in the absence of TCR engagement, we sought to determine to what extent the cysteine protease papain or LPS alone could alter the functional phenotype of the NP-specific CD4⁺ T cell population in the lung (Robinson et al., 1997; Guo et al., 2009, 2015; Fig. 5 A).

We found that after acute challenge with LPS, there was no difference in either the percent of T-bet–expressing or ST2-expressing cells in the lung-resident NP-specific CD4⁺ $T_{RM}$ population (Fig. 5, B and C). However, after acute challenge with papain, the NP-specific CD4⁺ $T_{RM}$ population exhibited a reduced frequency of T-bet expression and an increase in the frequency of ST2⁺ cells, suggesting that specific components of HDM that induce IL-33 expression may drive the phenotypic changes in the NP-specific CD4⁺ $T_{RM}$ in the lung after allergic challenge (Fig. 5, B and C). Together, these data suggest that papain but not LPS exposure is sufficient to induce a decreased frequency of T-bet and increased frequency of ST2 expression in the NP-specific CD4⁺ $T_{RM}$ population in the lung, recapitulating what we observed with HDM administration.

We next assessed whether either the direct administration of exogenous rIL-33 or rIL-18 could modulate the frequency of T-bet expression in the lung-resident NP-specific CD4⁺ $T_{RM}$ population. To determine this, we administered rIL-33 or rIL-18 to the lower respiratory tract beginning 25 d after PR8 infection (Fig. 5 D). Following cytokine challenge, we observed that rIL-33 but not rIL-18 was sufficient to reduce the frequency of T-bet expression in NP-specific CD4⁺ $T_{RM}$ in the lungs compared with unchallenged mice, although challenge with either of these cytokines was not sufficient to alter the overall frequency of ST2⁺ cells in this population at this time point (Fig. 5, E and F). Taken together, these data suggest that administration of rIL-33, but

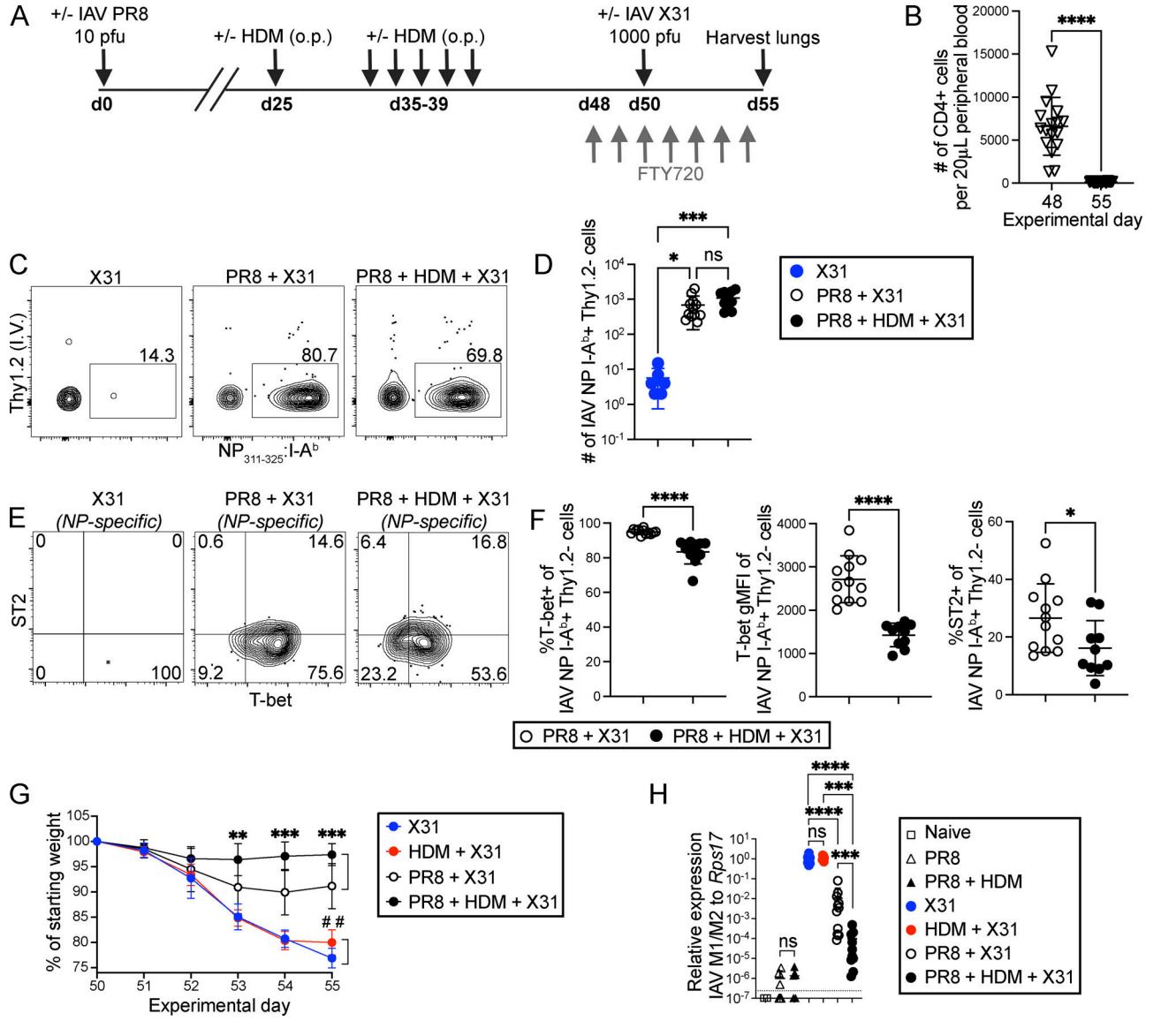


Figure 4. **HDM-exposed NP-specific CD4⁺ $T_{RM}$ maintain decreased T-bet expression after heterosubtypic infection and are associated with improved disease severity. (A)** Schematic of the experimental timeline for data in B–H. **(B)** The total number of CD4⁺ cells per 20 µl peripheral blood of mice at experimental day 48 prior to FTY720 administration and on day 55 prior to sacrifice. Data are pooled from 17–23 mice per time point from three independent experiments. **(C)** Representative flow cytometry plots of cells isolated from the lung at experimental day 55. Box gate denotes the Thy1.2⁻ NP-specific CD4⁺ cells in E. **(D)** Summary data of the number of NP-specific CD4⁺ cells in the lung at experimental day 55 as represented in C. Data are pooled from 6–12 mice per group from three independent experiments. **(E)** Representative flow cytometry plots of NP-specific CD4⁺ T cells isolated from the lung at experimental day 55. **(F)** Summary data of the percentage of T-bet⁺ NP-specific cells, the geometric mean fluorescence intensity of T-bet in NP-specific cells, and the percentage of ST2⁺ NP-specific cells as represented in E. Data are pooled from 10–12 mice per group from three independent experiments. **(G)** Graph summarizing morbidity following X31 infection as a percent of starting (experimental day 50) weight. Data are pooled from 2–12 mice per group from five independent experiments. **(H)** Quantification of viral load in whole lung tissue at experimental day 55 as measured by qRT-PCR. The dotted line indicates limit of detection. Data are pooled from 2–12 mice per group from five independent experiments. *, P < 0.05; ## or **, P < 0.01; ***, P < 0.001; ****, P < 0.0001. Graphs show mean ± SD. Data in B, D, F, and G were analyzed by unpaired *t* test. Data in H were analyzed by Mann–Whitney test. pfu, plaque-forming units. IAV, influenza A virus. o.p., oropharyngeal. gMFI, geometric mean fluorescence intensity.

not rIL-18, is sufficient to drive a decreased frequency of T-bet–expressing NP-specific CD4⁺ $T_{RM}$ in the lung.

To further assess the role of IL-33 in driving a decreased frequency of T-bet in NP-specific CD4⁺ $T_{RM}$ following HDM exposure, we utilized mice containing loxP sites flanking *Il1rl1* ($ST2^{flox/flox}$) and a tamoxifen-inducible Cre recombinase under control of the CD4 promoter ($CD4CreER^{T2+/-}$) to temporally delete ST2 expression in CD4⁺ T cells (Fig. 5 G). Injection of tamoxifen following PR8 infection but prior to HDM exposure selectively ablated ST2 expression in the CD4⁺ T cell compartment in the lungs of $CD4CreER^{T2+/-}$ $ST2^{flox/flox}$ mice, whereas littermates that did not possess a copy of the $CD4CreER^{T2}$ construct retained ST2 expression (Fig. 5 H). NP-specific CD4⁺ $T_{RM}$ isolated from $ST2^{flox/flox}$ control mice exhibited a reduced

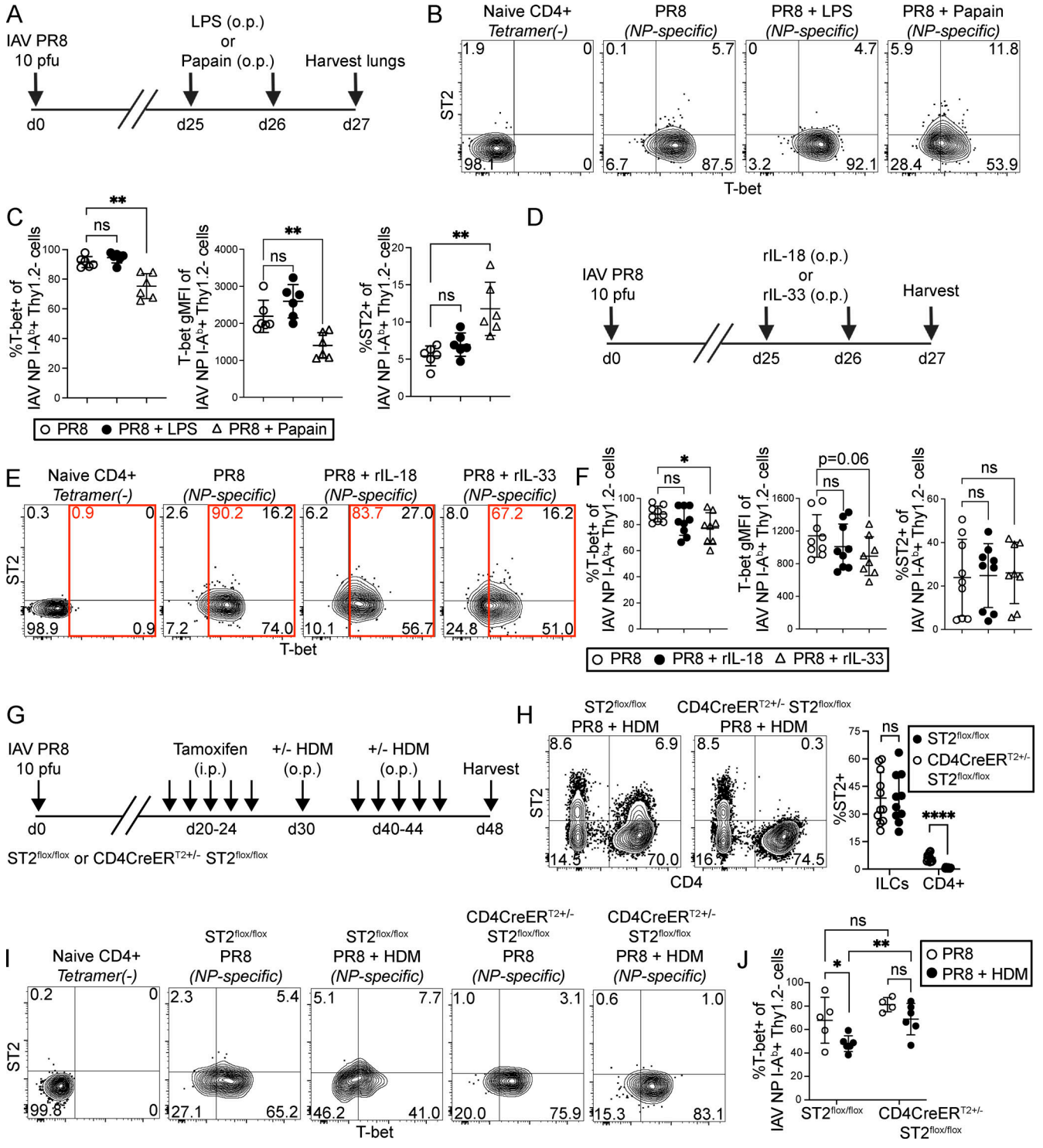


Figure 5. **Diminished T-bet expression in NP-specific CD4⁺ $T_{RM}$ in the lung can be driven by IL-33 and is dependent on ST2 signaling in CD4⁺ T cells.** **(A)** Schematic of the experimental timeline for data in B–C. **(B)** Representative flow cytometry plots of CD4⁺ T cells isolated from the lung at experimental day 27. **(C)** Summary data of the percentage of T-bet⁺ NP-specific cells, the geometric mean fluorescence intensity of T-bet in NP-specific cells, and the percentage of ST2⁺ NP-specific cells as represented in B. Data are pooled from six mice per group from two independent experiments. **(D)** Schematic of the experimental timeline for data in E and F. **(E)** Representative flow cytometry plots of CD4⁺ T cells isolated from the lung on experimental day 27. Red box gate and numbers define the T-bet⁺ population and associated frequency, respectively. **(F)** Summary data of the percentage of T-bet⁺ NP-specific cells, the geometric mean fluorescence intensity of T-bet in NP-specific cells, and the percentage of ST2⁺ NP-specific cells as represented in E. Data are pooled from eight to nine mice per group from three independent experiments. **(G)** Schematic of the experimental timeline for data in H–J. **(H)** Representative flow cytometry plots and summary data of ST2 expression by CD4⁺ and CD4⁻ cells isolated from the lung at experimental day 48. Plots are pregated on CD45.2⁺, B220⁻, CD8⁻, CD19⁻, F4/80⁻, CD11b⁻, CD11c⁻, TCR γΔ⁻, and NKG2d⁻ cells. Data are pooled from 10–11 mice per group from three independent experiments. **(I)** Representative flow cytometry plots of CD4⁺ T cells isolated from the lung at experimental day 48. **(J)** Summary data of the percentage of T-bet⁺ NP-specific cells as represented in I. Data are pooled from 10–11 mice per group from three independent experiments. *, P < 0.05; **, P < 0.01; ****, P < 0.0001. Graphs show mean ± SD and data were analyzed by unpaired *t* test. pfu, plaque-forming units. IAV, influenza A virus. o.p., oropharyngeal. gMFI, geometric mean fluorescence intensity.

frequency of T-bet expression after HDM exposure, similar to what was observed in wild-type mice (Fig. 5, I and J). However, CD4CreER$^{T2+/-}$ ST2$^{flox/flox}$ mice that had ST2 ablated in the CD4$^+$ compartment prior to challenge with HDM did not exhibit a significantly reduced frequency of T-bet expression in NP-specific CD4$^+$ $T_{RM}$ (Fig. 5, I and J). Thus, in addition to rIL-33 being sufficient to drive diminished T-bet expression in NP-specific CD4$^+$ $T_{RM}$, IL-33 receptor signaling in CD4$^+$ T cells is necessary for NP-specific lung $T_{RM}$ cells to decrease T-bet expression in response to HDM exposure.

### Concluding remarks

Our data demonstrate that a population of NP-specific CD4$^+$ Th1 $T_{RM}$ in the lung formed following influenza infection can be phenotypically and functionally altered by respiratory HDM or IL-33 exposure in an ST2-dependent manner. These changes in the overall composition of the lung-resident NP-specific CD4$^+$ T cells may reflect changes in the overall population as opposed to suggesting alterations in the expression of T-bet and ST2 at the individual cell level. For example, the loss of T-bet$^+$ cells due to lung egress in conjunction with the entry of T-bet$^-$ cells would lead to similar conclusions, as we did not observe an increase in the number of influenza-specific CD4$^+$ T cells in the lung after challenge with HDM. Notwithstanding, we have demonstrated that the modulation of this compartment is persistent and impacts memory cell functionality. In addition, while we demonstrate that reduced T-bet expression in NP-specific CD4$^+$ $T_{RM}$ responding to HDM exposure depends upon the expression of ST2 in CD4$^+$ T cells, further investigation is necessary to determine the exact relay of signals. NP-specific CD4$^+$ $T_{RM}$ may be directly perceiving IL-33 through ST2, leading to T-bet down-regulation, or perhaps ST2 signaling in HDM-specific CD4$^+$ T cells present during the allergic challenge phase drives alterations in the NP-specific population through paracrine cytokine production or other mechanisms. Although acute challenge with papain or rIL-33 over 2 d was sufficient to reduce the frequency of T-bet$^+$ NP-specific CD4$^+$ $T_{RM}$ prior to the formation of an allergen-specific population in the lungs, future investigation into the ST2-dependent mechanisms driving these observations should be performed.

The present findings also demonstrate that a lower frequency of T-bet$^+$ NP-specific CD4$^+$ $T_{RM}$ persists after cessation of allergic challenge and is associated with improved morbidity and reduced viral load and inflammatory cytokines upon heterosubtypic infection. While NP-specific CD4$^+$ $T_{RM}$ have been shown to be important for protection against influenza infection, some studies have suggested that CD4$^+$ Th1 cells can also promote pathology or worsen disease in response to heterosubtypic challenge with influenza (Teijaro et al., 2010, 2011; Schmit et al., 2022; McKinstry et al., 2019). Specifically, the production of IFN-γ in influenza infection promotes an antiviral response but is also associated with increased lung injury and weight loss (Schmit et al., 2022). Similarly, mice possessing IL-2–deficient memory CD4$^+$ T cells produce less cytokines, including IFN-γ and IL-12, during heterosubtypic influenza challenge and exhibit reduced morbidity and mortality (McKinstry et al., 2019). As we observed reduced expression of IFN-γ, and to a lesser degree, less IL-10 production in HDM-exposed NP-specific CD4$^+$ $T_{RM}$ upon reactivation, further investigation into the direct contribution of NP-specific CD4$^+$ $T_{RM}$-derived cytokines and other changes in this population on disease outcomes upon reinfection is necessary. In conclusion, these studies demonstrate that antigen-specific CD4$^+$ Th1 $T_{RM}$ populations in the lung are impacted by subsequent non-cognate local immune responses in an ST2-dependent, CD4$^+$ T cell–intrinsic manner, which may have important implications in future vaccine and therapeutic development.

## Materials and methods

### Mice

Female C57BL/6J mice, Red5 (B6(C)-Il5$^{tm1.1(icre)Lky}$/J) mice (#030926; JAX stock), Great "IFN-γ YFP" (C.129S4(B6)-Ifng$^{tm3.1Lky}$/J) mice (#017580; JAX stock), and CD4CreER$^{T2}$ (B6(129X1)-Tg(Cd4-cre/ERT2)11Gnri/J) mice were purchased from The Jackson Laboratory. ST2$^{flox/flox}$ mice were obtained from Steven Ziegler (Benaroya Research Institute, Seattle, WA, USA). CD4CreER$^{T2-/-}$ ST2$^{flox/flox}$ mice were bred to CD4CreER$^{T2+/-}$ ST2$^{flox/flox}$ mice and the resulting littermates were used for the indicated experiments. Mice that were infected with influenza A virus PR8 or influenza A virus X31 were housed in Animal Biosafety Level-2 conditions. All mice were maintained under specific pathogen–free conditions at the University of Washington. Experiments were performed in accordance with the University of Washington Institutional Animal Care and Use Committee guidelines.

For tamoxifen administration, 100 µl of an 11 mg/ml solution of tamoxifen (cat. no. T5648; Sigma-Aldrich) dissolved in 11% sterile EtOH and 89% sterile corn oil (cat. no. CO136; Spectrum Chemical) was administered to mice via intraperitoneal injection with a 25-gauge needle daily for 5 d.

### Viral infections

Mice were anesthetized with ketamine/xylazine and intranasally instilled with 10 plaque-forming units of influenza A virus PR8 or 1,000 plaque-forming units of influenza A virus X31 diluted in sterile PBS in a final volume of 40 µl. For experiments that utilized FTY720 (Fingolomod; Enzo Life Sciences), mice were injected intraperitoneally daily for the indicated range with 25 µg FTY720 in sterile deionized $H_20$.

### Immunizations

For preparation of HDM immunizations, whole crushed *D. pteronyssinus* HDM powder (Greer Laboratories Inc.) was resuspended in sterile PBS. For experiments that performed allergic sensitization and challenge, mice were anesthetized with isofluorane and administered HDM via the oropharynx at a concentration containing 23 µg Der p 1 protein in a volume of 40 µl during the primary sensitization. Beginning at 10 d after sensitization, mice were anesthetized with isofluorane and instilled with HDM in the oropharynx at a concentration containing 5.75 µg Der p 1 protein daily for 5 d during the allergic challenge phase.

For acute respiratory challenge experiments with HDM, papain, LPS, and recombinant cytokines, mice were anesthetized

with isofluorane and administered the target molecules in a total volume of 40 µl diluted in sterile PBS via the oropharynx for the indicated days. On each day, mice were given HDM normalized to 5.75 µg Der p 1 protein (Greer Laboratories Inc.), 25 µg papain (from papaya latex, aseptically filled; Sigma-Aldrich), 10 µg Ultrapure LPS from *E. coli* O111:B4 (InvivoGen), 50 ng recombinant mouse IL-33 (BioLegend), and/or 500 ng recombinant mouse IL-18 (BioLegend) as described in the relevant figures.

### Isolation of cells from the lung

Approximately 3 min prior to sacrifice, mice were injected intravenously with 1 µg anti-Thy1.2 BUV395 (clone 53-2.1; BD Biosciences) to label T cells in the vasculature (Anderson et al., 2014). Mice were then euthanized via $CO_2$ asphyxiation and lungs were harvested in PBS with 2% fetal calf serum. The lung tissue was placed into gentleMACS C Tubes (Miltenyi Biotec) with RPMI 1640 Medium with Hepes (#22400089; Gibco) containing 70 µg/ml Liberase (#05401127001; Roche) and 10 mM aminoguanidine (cat. no. A7009; Sigma-Aldrich). The tissue was dissociated on the gentleMACS Dissociator (Miltenyi Biotec) and then incubated at 37°C for 30 min followed by a final dissociation step. The single-cell suspensions from the lung were then filtered over 70-µm mesh and washed with Dulbecco's Modified Eagle's Medium (Ref: 10-017-CV; Corning, Inc.) with 10% fetal calf serum to inhibit liberase activity.

### Quantitative reverse transcription PCR (qRT-PCR)

For viral RNA quantification, the right middle lung lobe was harvested from C57BL/6J mice and placed in RNAlater Stabilization Solution (Invitrogen) at −20°C. 15 mg of lung tissue was lysed using the RNeasy Plus Mini Kit RLT buffer with β-mercaptoethanol (Qiagen) and a 5-mm stainless steel bead (Qiagen) on the TissueLyser II (Qiagen) twice for 2.3 min at 30 Hz. RNA was isolated from the lysate using the RNeasy Plus Mini Kit (Qiagen) according to manufacturer instructions. Isolated RNA was then synthesized and amplified into cDNA using the High-Capacity cDNA Reverse Transcription Kit (Thermo Fisher Scientific). For influenza A virus M1/M2 transcript measurement, this cDNA was used as a template for quantitative PCR using Prime Time qPCR Probe Assays (Integrated DNA Technologies, Inc.) and Prime Time Gene Expression Master Mix (Integrated DNA Technologies, Inc.) with the following primer and probe design: Probe: (6-FAM/ZEN/IBFQ) 5′-CCTCTG CTGCTTGCTCACTCGATC-3′; Forward Primer: 5′-CAGCACTAC AGCTAAGGCTATG-3′; Reverse Primer: 5′-CTCATCGCTTGCACC ATTTG-3′. Transcripts were normalized to *Rps17* (40S ribosomal protein S17) which was quantified using PowerUP SYBR Green Master Mix (Applied Biosystems) with the primers: *Rps17* Fwd: 5′-CGCCATTATCCCCAGCAAG-3′; *Rps17* Rev: 5′-TGTCGGGAT CCACCTCAATG-3′. For IL-6, IFN-γ, and TNF-α quantification, the following primers were used with PowerUP SYBR Green Master Mix and normalized to *Rps17*. *Il6* Fwd: 5′-TGAACAACG ATGATGCACTTG-3′; *Il6* Rev: 5′-CTGAAGGACTCTGGCTTTGTC-3′; *Ifng* Fwd: 5′-ATGAACGCTACACACTGCATC-3′; *Ifng* Rev: 5′-CCATCCTTTTGCCAGTTCCTC-3′; *Tnf* Fwd: 5′-TCTGTCTACTGA ACTTCGGGGTG-3′; *Tnf* Rev: 5′-ACTTGGTGGTTTGCTACGACG-3′. Quantitation was performed on the ViiA7 Real-Time PCR System (Applied Biosystems).

### In vitro stimulation and intracellular cytokine staining

After acquiring a single-cell suspension from lung tissue digestion (see Isolation of cells from the lung), cells were pelleted and resuspended in 25 ng/ml PMA and 1.4 µM Ionomycin in Dulbecco's Modified Eagle's Medium (Ref: 10-017-CV; Corning, Inc.) with 10% fetal calf serum for 4.5 h at 37°C. For the final 3.5 h of culture, BD GolgiStop (BD Biosciences) containing Monensin was added according to manufacturer instructions. Following incubation, the cells were filtered over nitex mesh (https://amazon.com) and stained with APC-conjugated $NP_{311–325}$:I-$A^b$ tetramer for 1 h at room temperature. Cells were then washed and stained for surface markers (CD4, clone: GK1.5; BD Biosciences; B220, clone: RA3-6B2; BD Biosciences; LIVE/DEAD Fixable Blue Dead Cell Stain Kit, Invitrogen; Purified CD16/CD32, clone 2.4G2; BD Biosciences) for 30 min on ice. Cells were then fixed and permeabilized with eBioscience Foxp3/Transcription Factor Staining Buffer Set (Invitrogen) according to manufacturer instructions. Intracellular cytokine staining (IFN-γ, clone: XMG1.2; BioLegend; IL-10, clone JES5-16E3; BioLegend; IL-13, clone eBio13A; Invitrogen) was performed in 1X Permeabilization Buffer (Invitrogen) at room temperature for 1 h before flow cytometry acquisition.

### Cell enrichment and flow cytometry

Following acquisition of single-cell suspensions, cells were stained with $NP_{311–325}$ (QVYSLIRPNENPAHK) I-$A^b$ tetramer or Der p $1_{117–127}$ (CQIYPPNVNKI) I-$A^b$ as indicated conjugated to APC or PE and incubated at room temperature in the dark for 1 h. Cells were then washed and incubated with 25 µl anti-APC and/or anti-PE microbeads (Miltenyi Biotec) on ice for 30 min. After incubation, cells were washed and tetramer-positive cells were enriched over magnetic LS columns (Miltenyi Biotec) as previously described (Moon et al., 2007; Legoux and Moon 2012). The enriched fraction and "flow-through" non-enriched fraction were then surface-stained with identical antibody master mixes on ice for 30 min for downstream analysis of tetramer-specific cells and bulk lymphocyte populations. When applicable, cells were then fixed and permeabilized with eBioscience Foxp3/Transcription Factor Staining Buffer Set (Invitrogen) according to manufacturer instructions. Intracellular transcription factor staining was performed in 1X Permeabilization Buffer (Invitrogen) at room temperature for 1 h before data acquisition by flow cytometry. All cells were acquired on the LSR II or FACSymphony (BD) and analyzed using FlowJo 10.8.1 software (Treestar). All plots shown in figures are pregated on FSCxSSC singlet $B220^-$ $CD8^-$ $CD4^+$ cells. Naïve $CD4^+$ cells as indicated are further gated on $CD62L^+$ $CD44^-$ $CD69^-$ cells.

For surface staining, the following antibodies were used: B220 (clone: RA3-6B2; BD), CD4 (clone: RM4-5 or GK1.5; BioLegend or BD), CD8 (clone: 53-6.7; BD), CD3 (clone: 145-2C11; BD), CD44 (clone: IM7; BD), CD69 (clone: H1.2F3; BD), CD62L (clone: MEL-14; BD), CD218a (clone: P3TUNYA; Invitrogen), ST2 (clone: DJ8; MD Bioproducts), Thy1.2 (clone: 53-2.1; BD), CD45.2 (clone: 104; eBioscience), CD19 (clone: eBio1D3; eBioscience), F4/80 (clone: BM8; BioLegend), NKG2d (clone: CX5; eBioscience), TCR γΔ (clone: eBioGL3; eBioscience), CD11b (clone: M1/70; BD), and CD11c (clone: N418; BioLegend). For intracellular transcription

factor staining, the following antibodies were used: T-bet (clone: 4B10; Invitrogen), GATA3 (clone: L50-823; BD), and Foxp3 (clone: FJK-16s; Invitrogen).

### Statistical analysis

Statistical analysis was performed by unpaired *t* test, Mann–Whitney test, Spearman's rank correlation, and tested for normality by Shapiro–Wilk test as indicated in the figure legends using Prism 9.5.1 (GraphPad Software). Graphs show mean ± SD.

### Online supplemental material

Fig. S1 demonstrates *Ifng* and *Il6*, but not *Tnf*, transcript levels in the lung on day 5 after X31 infection are reduced if mice previously infected with PR8 were additionally exposed to HDM prior to heterosubtypic challenge. Furthermore, the level of *Ifng* and *Il6* transcript in the lung, as well as T-bet expression in NP-specific $CD4^+$ $T_{RM}$, positively correlates with viral load on day 5 following challenge with X31. Fig. S2 demonstrates that NP-specific $CD4^+$ $T_{RM}$ in the lung express IL-18Ra after PR8 infection and are upregulated following challenge with LPS but not papain.

### Data availability

Data are available in the article or upon a reasonable request to the corresponding author.

## Acknowledgments

We thank Paul Thomas (St. Jude Children's Research Hospital, Memphis, TN, USA) and Andrew Oberst (University of Washington, Seattle, WA, USA) for influenza virus stocks. We express gratitude to Daniel J. Campbell, Steven F. Ziegler (Benaroya Research Institute, Seattle, WA, USA), Jakob von Moltke, and William Altemeier (University of Washington, Seattle, WA, USA) for their considerable feedback and helpful discussions. The Cell Analysis Facility at the University of Washington provided advice and equipment for flow cytometry data acquisition. The schematics of experimental timelines in some figures were created with BioRender.com.

Funding for the BD FACSymphony cytometer was supported by the National Institutes of Health grant 1S10OD024979-01A1. This work was supported by the National Institutes of Health (grant U19 A107422), and M.J. Rüterbusch was supported by the National Institutes of Health training grant TL1 TR002318.

Author contributions: M.J. Rüterbusch conceptualized the study, designed and performed experiments, analyzed the data, and wrote the manuscript. B.D. Hondowicz and K.B. Pruner designed experiments and provided expertise in flow cytometry. K.K. Takehara performed experiments and generated reagents. T.S. Griffith supplied reagents, provided expertise in tetramer production, and revised the manuscript. M. Pepper conceptualized the study, designed experiments, analyzed the data, and wrote the manuscript.

Disclosures: M. Pepper is on the Vaxart Scientific Advisory Board, but there is no conflict of interest. No other disclosures were reported.

Submitted: 17 January 2023
Revised: 11 July 2023
Accepted: 22 August 2023

## References

Anderson, K.G., K. Mayer-Barber, H. Sung, L. Beura, B.R. James, J.J. Taylor, L. Qunaj, T.S. Griffith, V. Vezys, D.L. Barber, and D. Masopust. 2014. Intravascular staining for discrimination of vascular and tissue leukocytes. *Nat. Protoc.* 9:209–222. https://doi.org/10.1038/nprot.2014.005

Baumann, C., W.V. Bonilla, A. Fröhlich, C. Helmstetter, M. Peine, A.N. Hegazy, D.D. Pinschewer, and M. Löhning. 2015. T-bet- and STAT4-dependent IL-33 receptor expression directly promotes antiviral Th1 cell responses. *Proc. Natl. Acad. Sci. USA*. 112:4056–4061. https://doi.org/10.1073/pnas.1418549112

Belz, G.T., D. Wodarz, G. Diaz, M.A. Nowak, and P.C. Doherty. 2002. Compromised influenza virus-specific CD8(+)-T-cell memory in CD4(+)-T-cell-deficient mice. *J. Virol.* 76:12388–12393. https://doi.org/10.1128/JVI.76.23.12388-12393.2002

Blom, L., and L.K. Poulsen. 2012. IL-1 family members IL-18 and IL-33 upregulate the inflammatory potential of differentiated human Th1 and Th2 cultures. *J. Immunol.* 189:4331–4337. https://doi.org/10.4049/jimmunol.1103685

Cabrera-Perez, J., S.A. Condotta, B.R. James, S.W. Kashem, E.L. Brincks, D. Rai, T.A. Kucaba, V.P. Badovinac, and T.S. Griffith. 2015. Alterations in antigen-specific naive CD4 T cell precursors after sepsis impairs their responsiveness to pathogen challenge. *J. Immunol.* 194:1609–1620. https://doi.org/10.4049/jimmunol.1401711

Califano, D., Y. Furuya, S. Roberts, D. Avram, A.N.J. McKenzie, and D.W. Metzger. 2018. IFN-γ increases susceptibility to influenza A infection through suppression of group II innate lymphoid cells. *Mucosal Immunol.* 11:209–219. https://doi.org/10.1038/mi.2017.41

Crowe, S.R., S.C. Miller, D.M. Brown, P.S. Adams, R.W. Dutton, A.G. Harmsen, F.E. Lund, T.D. Randall, S.L. Swain, and D.L. Woodland. 2006. Uneven distribution of MHC class II epitopes within the influenza virus. *Vaccine*. 24:457–467. https://doi.org/10.1016/j.vaccine.2005.07.096

Daan de Boer, J., J.J.T.H. Roelofs, A.F. de Vos, R. de Beer, M. Schouten, T.J. Hommes, A.J. Hoogendijk, O.J. de Boer, I. Stroo, J.S. van der Zee, et al. 2013. Lipopolysaccharide inhibits Th2 lung inflammation induced by house dust mite allergens in mice. *Am. J. Respir. Cell Mol. Biol.* 48:382–389. https://doi.org/10.1165/rcmb.2012-0331OC

Felgenhauer, J.L., J.E. Brune, M.E. Long, A.M. Manicone, M.Y. Chang, T.L. Brabb, W.A. Altemeier, and C.W. Frevert. 2020. Evaluation of nutritional gel supplementation in C57BL/6J mice infected with mouse-adapted influenza A/PR/8/34 virus. *Comp. Med.* 70:471–486. https://doi.org/10.30802/AALAS-CM-20-990138

Finotto, S., M.F. Neurath, J.N. Glickman, S. Qin, H.A. Lehr, F.H.Y. Green, K. Ackerman, K. Haley, P.R. Galle, S.J. Szabo, et al. 2002. Development of spontaneous airway changes consistent with human asthma in mice lacking T-bet. *Science*. 295:336–338. https://doi.org/10.1126/science.1065544

Geginat, J., F. Sallusto, and A. Lanzavecchia. 2001. Cytokine-driven proliferation and differentiation of human naive, central memory, and effector memory CD4(+) T cells. *J. Exp. Med.* 194:1711–1719. https://doi.org/10.1084/jem.194.12.1711

Guo, L., G. Wei, J. Zhu, W. Liao, W.J. Leonard, K. Zhao, and W. Paul. 2009. IL-1 family members and STAT activators induce cytokine production by Th2, Th17, and Th1 cells. *Proc. Natl. Acad. Sci. USA*. 106:13463–13468. https://doi.org/10.1073/pnas.0906988106

Guo, L., Y. Huang, X. Chen, J. Hu-Li, J.F. Urban Jr, and W.E. Paul. 2015. Innate immunological function of TH2 cells in vivo. *Nat. Immunol.* 16:1051–1059. https://doi.org/10.1038/ni.3244

Hondowicz, B.D., D. An, J.M. Schenkel, K.S. Kim, H.R. Steach, A.T. Krishnamurty, G.J. Keitany, E.N. Garza, K.A. Fraser, J.J. Moon, et al. 2016. Interleukin-2-Dependent allergen-specific tissue-resident memory cells drive asthma. *Immunity*. 44:155–166. https://doi.org/10.1016/j.immuni.2015.11.004

Jain, A., R. Song, E.K. Wakeland, and C. Pasare. 2018. T cell-intrinsic IL-1R signaling licenses effector cytokine production by memory CD4 T cells. *Nat. Commun.* 9:3185. https://doi.org/10.1038/s41467-018-05489-7

Laidlaw, B.J., N. Zhang, H.D. Marshall, M.M. Staron, T. Guan, Y. Hu, L.S. Cauley, J. Craft, and S.M. Kaech. 2014. CD4+ T cell help guides formation of CD103+ lung-resident memory CD8+ T cells during influenza viral

infection. *Immunity*. 41:633–645. https://doi.org/10.1016/j.immuni.2014.09.007

Legoux, F.P., and J.J. Moon. 2012. Peptide:MHC tetramer-based enrichment of epitope-specific T cells. *J. Vis. Exp.* 68:4420. https://doi.org/10.3791/4420

Löhning, M., A. Stroehmann, A.J. Coyle, J.L. Grogan, S. Lin, J.C. Gutierrez-Ramos, D. Levinson, A. Radbruch, and T. Kamradt. 1998. T1/ST2 is preferentially expressed on murine Th2 cells, independent of interleukin 4, interleukin 5, and interleukin 10, and important for Th2 effector function. *Proc. Natl. Acad. Sci. USA*. 95:6930–6935. https://doi.org/10.1073/pnas.95.12.6930

Mandala, S., R. Hajdu, J. Bergstrom, E. Quackenbush, J. Xie, J. Milligan, R. Thornton, G.J. Shei, D. Card, C. Keohane, et al. 2002. Alteration of lymphocyte trafficking by sphingosine-1-phosphate receptor agonists. *Science*. 296:346–349. https://doi.org/10.1126/science.1070238

Manigold, T., U. Böcker, P. Traber, T. Dong-Si, M. Kurimoto, C. Hanck, M.V. Singer, and S. Rossol. 2000. Lipopolysaccharide/endotoxin induces IL-18 via CD14 in human peripheral blood mononuclear cells in vitro. *Cytokine*. 12:1788–1792. https://doi.org/10.1006/cyto.2000.0783

Mantovani, A., C.A. Dinarello, M. Molgora, and C. Garlanda. 2019. Interleukin-1 and related cytokines in the regulation of inflammation and immunity. *Immunity*. 50:778–795. https://doi.org/10.1016/j.immuni.2019.03.012

McKinstry, K.K., F. Alam, V. Flores-Malavet, M.Z. Nagy, S. Sell, A.M. Cooper, S.L. Swain, and T.M. Strutt. 2019. Memory CD4 T cell-derived IL-2 synergizes with viral infection to exacerbate lung inflammation. *PLoS Pathog.* 15:e1007989. https://doi.org/10.1371/journal.ppat.1007989

Moon, J.J., H.H. Chu, M. Pepper, S.J. McSorley, S.C. Jameson, R.M. Kedl, and M.K. Jenkins. 2007. Naive CD4(+) T cell frequency varies for different epitopes and predicts repertoire diversity and response magnitude. *Immunity*. 27:203–213. https://doi.org/10.1016/j.immuni.2007.07.007

Nussbaum, J.C., S.J. Van Dyken, J. von Moltke, L.E. Cheng, A. Mohapatra, A.B. Molofsky, E.E. Thornton, M.F. Krummel, A. Chawla, H.E. Liang, and R.M. Locksley. 2013. Type 2 innate lymphoid cells control eosinophil homeostasis. *Nature*. 502:245–248. https://doi.org/10.1038/nature12526

Obst, R., H.M. van Santen, D. Mathis, and C. Benoist. 2005. Antigen persistence is required throughout the expansion phase of a CD4(+) T cell response. *J. Exp. Med.* 201:1555–1565. https://doi.org/10.1084/jem.20042521

Pepper, M., J.L. Linehan, A.J. Pagán, T. Zell, T. Dileepan, P.P. Cleary, and M.K. Jenkins. 2010. Different routes of bacterial infection induce long-lived TH1 memory cells and short-lived TH17 cells. *Nat. Immunol.* 11:83–89. https://doi.org/10.1038/ni.1826

Reinhardt, R.L., H.E. Liang, and R.M. Locksley. 2009. Cytokine-secreting follicular T cells shape the antibody repertoire. *Nat. Immunol.* 10:385–393. https://doi.org/10.1038/ni.1715

Robinson, D., K. Shibuya, A. Mui, F. Zonin, E. Murphy, T. Sana, S.B. Hartley, S. Menon, R. Kastelein, F. Bazan, and A. O'Garra. 1997. IGIF does not drive Th1 development but synergizes with IL-12 for interferon-gamma production and activates IRAK and NFkappaB. *Immunity*. 7:571–581. https://doi.org/10.1016/S1074-7613(00)80378-7

Rutigliano, J.A., S. Sharma, M.Y. Morris, T.H. Oguin 3rd, J.L. McClaren, P.C. Doherty, and P.G. Thomas. 2014. Highly pathological influenza A virus infection is associated with augmented expression of PD-1 by functionally compromised virus-specific CD8+ T cells. *J. Virol.* 88:1636–1651. https://doi.org/10.1128/JVI.02851-13

Schmit, T., K. Guo, J.K. Tripathi, Z. Wang, B. McGregor, M. Klomp, G. Ambigapathy, R. Mathur, J. Hur, M. Pichichero, et al. 2022. Interferon-γ promotes monocyte-mediated lung injury during influenza infection. *Cell Rep.* 38:110456. https://doi.org/10.1016/j.celrep.2022.110456

Schmitz, J., A. Owyang, E. Oldham, Y. Song, E. Murphy, T.K. McClanahan, G. Zurawski, M. Moshrefi, J. Qin, X. Li, et al. 2005. IL-33, an interleukin-1-like cytokine that signals via the IL-1 receptor-related protein ST2 and induces T helper type 2-associated cytokines. *Immunity*. 23:479–490. https://doi.org/10.1016/j.immuni.2005.09.015

Scott, I.C., J.B. Majithiya, C. Sanden, P. Thornton, P.N. Sanders, T. Moore, M. Guscott, D.J. Corkill, J.S. Erjefält, and E.S. Cohen. 2018. Interleukin-33 is activated by allergen- and necrosis-associated proteolytic activities to regulate its alarmin activity during epithelial damage. *Sci. Rep.* 8:3363. https://doi.org/10.1038/s41598-018-21589-2

Son, Y.M., I.S. Cheon, Y. Wu, C. Li, Z. Wang, X. Gao, Y. Chen, Y. Takahashi, Y.X. Fu, A.L. Dent, et al. 2021. Tissue-resident CD4$^+$ T helper cells assist the development of protective respiratory B and CD8$^+$ T cell memory responses. *Sci. Immunol.* 6:eabb6852. https://doi.org/10.1126/sciimmunol.abb6852

Swarnalekha, N., D. Schreiner, L.C. Litzler, S. Iftikhar, D. Kirchmeier, M. Künzli, Y.M. Son, J. Sun, E.A. Moreira, and C.G. King. 2021. T resident helper cells promote humoral responses in the lung. *Sci. Immunol.* 6:eabb6808. https://doi.org/10.1126/sciimmunol.abb6808

Szabo, S.J., S.T. Kim, G.L. Costa, X. Zhang, C.G. Fathman, and L.H. Glimcher. 2000. A novel transcription factor, T-bet, directs Th1 lineage commitment. *Cell*. 100:655–669. https://doi.org/10.1016/S0092-8674(00)80702-3

Teijaro, J.R., D. Verhoeven, C.A. Page, D. Turner, and D.L. Farber. 2010. Memory CD4 T cells direct protective responses to influenza virus in the lungs through helper-independent mechanisms. *J. Virol.* 84:9217–9226. https://doi.org/10.1128/JVI.01069-10

Teijaro, J.R., D. Turner, Q. Pham, E.J. Wherry, L. Lefrançois, and D.L. Farber. 2011. Cutting edge: Tissue-retentive lung memory CD4 T cells mediate optimal protection to respiratory virus infection. *J. Immunol.* 187:5510–5514. https://doi.org/10.4049/jimmunol.1102243

Valerio, C.R., P. Murray, L.G. Arlian, and J.E. Slater. 2005. Bacterial 16S ribosomal DNA in house dust mite cultures. *J. Allergy Clin. Immunol.* 116:1296–1300. https://doi.org/10.1016/j.jaci.2005.09.046

Van Dyken, S.J., J.C. Nussbaum, J. Lee, A.B. Molofsky, H.E. Liang, J.L. Pollack, R.E. Gate, G.E. Haliburton, C.J. Ye, A. Marson, et al. 2016. A tissue checkpoint regulates type 2 immunity. *Nat. Immunol.* 17:1381–1387. https://doi.org/10.1038/ni.3582

Wan, H., H.L. Winton, C. Soeller, E.R. Tovey, D.C. Gruenert, P.J. Thompson, G.A. Stewart, G.W. Taylor, D.R. Garrod, M.B. Cannell, and C. Robinson. 1999. Der p 1 facilitates transepithelial allergen delivery by disruption of tight junctions. *J. Clin. Invest.* 104:123–133. https://doi.org/10.1172/JCI5844

Zhang, D.H., L. Cohn, P. Ray, K. Bottomly, and A. Ray. 1997. Transcription factor GATA-3 is differentially expressed in murine Th1 and Th2 cells and controls Th2-specific expression of the interleukin-5 gene. *J. Biol. Chem.* 272:21597–21603. https://doi.org/10.1074/jbc.272.34.21597

## Supplemental material

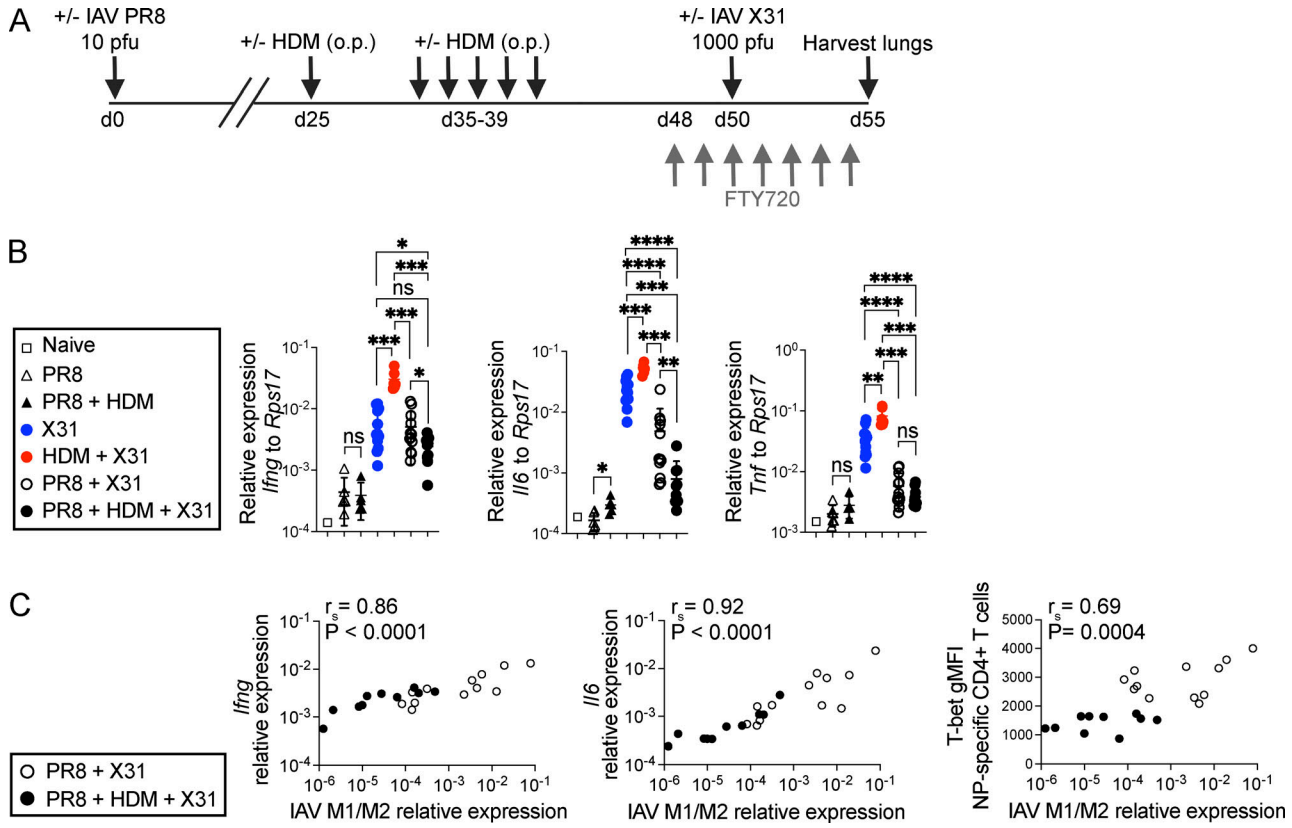


Figure S1. **Proinflammatory cytokine levels in the lung are reduced after heterosubtypic challenge in mice exposed to HDM following PR8 infection and positively correlate with increased viral load. (A)** Schematic of the experimental timeline for data in B. **(B)** Quantification of *Ifng*, *Il6*, and *Tnf* transcript expression in whole lung tissue on experimental day 55 as measured by qRT-PCR. Data are pooled from 1–12 mice per group from five independent experiments. **(C)** Correlation of viral transcript expression and *Ifng* expression in whole lung tissue, *Il6* expression in whole lung tissue, and level of T-bet expression in NP-specific $CD4^+$ T cells isolated from the lung on experimental day 55. *, $P < 0.05$; **, $P < 0.01$; ***, $P < 0.001$; ****, $P < 0.0001$. Graphs in B show mean ± SD. Data in B were analyzed by Mann–Whitney test, data in C were analyzed by Spearman's rank correlation. pfu, plaque-forming units. IAV, influenza A virus; o.p., oropharyngeal. gMFI, geometric mean fluorescence intensity.

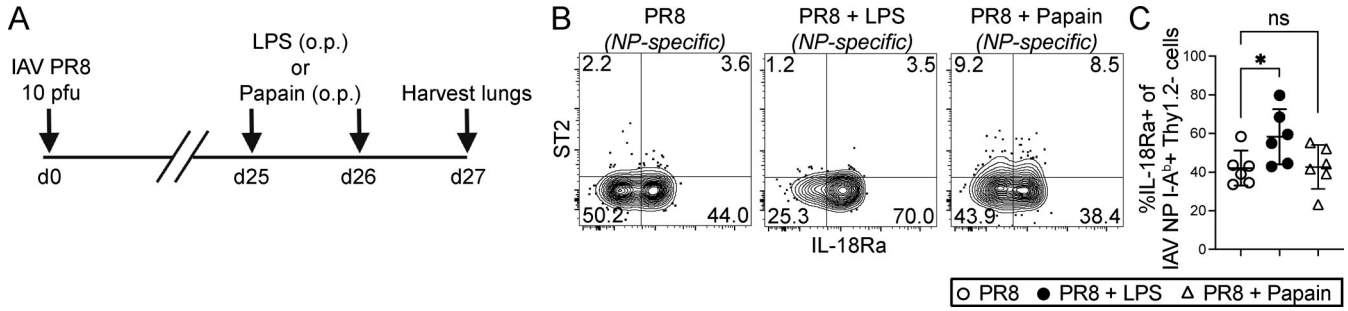


Figure S2. **NP-specific CD4⁺ $T_{RM}$ in the lung express IL-18Ra. (A)** Schematic of the experimental timeline for data in B and C. **(B)** Representative flow cytometry plots of CD4⁺ T cells isolated from the lung at experimental day 27. **(C)** Summary data of the percentage of IL-18Ra⁺ NP-specific cells as represented in B. Data are pooled from six mice per group from two independent experiments. *, P < 0.05. Graphs show mean ± SD and data were analyzed by unpaired *t* test. pfu, plaque-forming units. IAV, influenza A virus. o.p., oropharyngeal.